

Multi-epitope mRNA Vaccine Design that Exploits Variola Virus and Monkeypox Virus Proteins for Elicitation of Long-lasting Humoral and Cellular Protection Against Severe Disease

Dženan Kovačić

Department of Genetics and Bioengineering, Faculty of Engineering and Natural Sciences, International Burch University, Ilidža, Bosnia and Herzegovina

 <https://orcid.org/0000-0003-3218-5073>

Corresponding author: dzenan.kovacic@stu.ibu.edu.ba

Adna Salihović

Department of Genetics and Bioengineering, Faculty of Engineering and Natural Sciences, International Burch University, Ilidža, Bosnia and Herzegovina

 <https://orcid.org/0000-0003-0482-1861>

Keywords: smallpox, monkeypox, monkeypox outbreak, monkeypox vaccine, mRNA vaccines, poxviruses

Published: 2022-11-28

How to Cite: Kovačić D, Salihović A. Multi-epitope mRNA Vaccine Design that Exploits Variola Virus and Monkeypox Virus Proteins for Elicitation of Long-lasting Humoral and Cellular Protection Against Severe Disease. *Journal of Medical Science*. Ahead of Print. doi:10.20883/medical.e750

 DOI: <https://doi.org/10.20883/medical.e750>



© 2022 by the author(s). This is an open access article distributed under the terms and conditions of the Creative Commons Attribution (CC BY-NC) license. Published by Poznan University of Medical Sciences

ABSTRACT

Human monkeypox represents a relatively underexplored infection that has received increased attention since the reported outbreak in May 2022. Due to its clinical similarities with human smallpox, this virus represents a potentially tremendous health problem demanding further research in the context of host-pathogen interactions and vaccine development. Furthermore, the cross-continental spread of monkeypox has reaffirmed the need for devoting attention to human poxviruses in general, as they represent potential bioterrorism agents. Currently, smallpox vaccines are utilized in immunization efforts against monkeypox, an unsurprising fact considering their genomic and phenotypic similarities. Though it offers long-lasting protection against smallpox, its protective effects against human monkeypox continue to be explored, with encouraging results. Taking this into account, this work aims at utilizing *in silico* tools to identify potent peptide-based epitopes stemming from the variola virus and monkeypox virus proteomes, to devise a vaccine that would offer significant protection against smallpox and monkeypox. In theory, a vaccine that offers cross-protection against variola and monkeypox would also protect against related viruses, at least in severe clinical manifestation. Herein, we introduce a novel multi-epitope mRNA vaccine design that exploits these two viral proteomes to elicit long-lasting humoral and cellular immunity. Special consideration was taken in ensuring that the vaccine candidate elicits a Th1 immune response, correlated with protection against clinically severe disease for both viruses. Immune system simulations and physicochemical and safety analyses characterize our vaccine candidate as antigenically potent, safe, and overall stable. The protein product displays high binding affinity towards relevant immune receptors. Furthermore, the vaccine candidate is to elicit a protective, humoral and Th1-dominated cellular immune response that lasts over five years. Lastly, we build a case about the rapidity and convenience of circumventing the live attenuated vaccine platform using mRNA vaccine technology.

Background

A currently ongoing outbreak of the monkeypox virus (MPXV), a zoonotic orthopoxvirus, was reported by the World Health Organization in May 2022, with the initial cluster identified in the United Kingdom. Though characterized as a rare zoonosis, over 10,000 cases have been reported thus far across the world. Two well-characterized clades of MPXV exist (West African and Central African). However, the clade responsible for the 2022 outbreak is genomically distinct from the two clades. Additionally, monkeypox is clinically indistinguishable from smallpox, though the transmissibility and severity of monkeypox disease are lower than the latter. The distinction between monkeypox and smallpox arose only in the 1970s during the smallpox eradication program when the virus was isolated from a suspected smallpox patient. Considering that the causative agent of smallpox – the variola virus – was eradicated from the human population in the 1980s, surveilling and studying other zoonotic orthopoxviruses with similar or identical clinical manifestations is justifiably garnering increased attention. Currently approved monkeypox vaccines are not specifically targeted to the MPXV orthopoxvirus but to human variola. The fact is sensible, considering the overlapping clinical manifestations between these human infec-

tions and their genomic similarity. Observational studies have revealed that the smallpox vaccine derived from the Vaccinia virus is 85% effective at preventing monkeypox. A novel attenuated Vaccinia virus vaccine was approved for the prevention of monkeypox in 2019. However, the vaccine is modestly available across the world.

The host innate immune response against poxviruses can be generally described as a classic antiviral response; interferon (IFN), the complement system, natural killer, and inflammatory cells are all engaged, upon which a greater inflammatory response typically ensues. Humoral and cell-mediated immunity, in the case of MPXV infected cells, mount the adaptive immune response via antibody-dependent cell-mediated cytotoxicity, virus neutralization, opsonization, and cytotoxic T-lymphocyte (CTL) effector functions through a myriad of pattern recognition receptor (PRR) families [1]. Specifically, effective viral control correlates strongly with the generation of neutralizing antibodies; it has been shown that CD4+/CD8+ T lymphocytes are not necessary for recovery from secondary poxvirus infection and are depleted after 8–15 years upon vaccination (**Figure 1**) [2]. Furthermore, MPXV-infected cells are believed to be able to trigger a state of unresponsiveness of T cells and thus evade CTL effector functions in a major histocompatibility complex (MHC)-independent fashion [3].

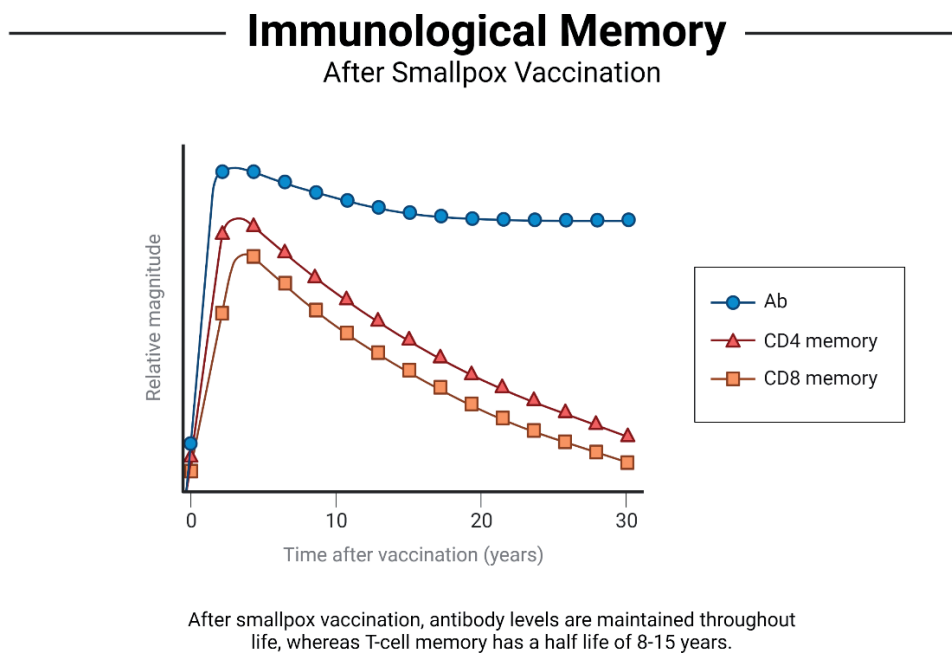


Figure 1. The canonical immune response to smallpox vaccination. Prepared based on data from [4–6]

The ability of poxviruses, primarily, to inhibit pro-inflammatory cytokines that regulate MHC expression (such as tumour necrosis factor (TNF) and IFN) may explain the indirect mechanisms at play that downplay the role of MHC. Considering the MPXV-infected intracellular environment, the inhibition of apoptosis via caspases and the protein kinase R (PKR) signalling pathway employs anti-IFN strategies. Indeed, the abrogation of IFN signalling was explored in further detail as a critical factor in promoting MPXV pathogenesis in humans [7]. MPXV encodes several PKR antagonists, notably, the MPXV F3 protein encoded by host genes F3L, a homolog of the VACV E3 protein homolog) that inhibits the PKR pathway [8]. Generally, the PRRs PKR and 2'-5'-oligoadenylate synthetase (OAS)/RNase L as the double-stranded RNA-activated sensors overarch the IFN-induced systems in response to MPXV infection [9]. The diverse crosstalk between several immune pathways with multiple PRRs targeting the same viral proteins mirrors the cascades of the viral antagonists, as alluded on the E3 sequestering dsRNA inhibiting PKR, OAS/RNase L, and Toll-like receptors (TLRs).

Ultimately, the importance of antibodies in MPXV infection was further heightened in a study realizing the insufficient protection from MPXV in immunodeficient macaques upon smallpox (Dryvax vaccine) immunization due to antibody-mediated depletion of B cells. To this end, utilisation of humoral immunity by using antigens that are targets of intracellular mature virions in neutralising antibodies is believed to warrant an effective monkeypox vaccine with an improved safety profile. Furthermore, smallpox vaccines' strong T and B cell responses target various viral proteins and offer cross-protective immunity against significant human infections, including variola and MPXV [4].

With mRNA vaccine technology recently finding its real-world applicational affirmation, utilizing this technology to devise more efficient vaccines has become an attractive notion. Though traditional vaccines garner a safety and efficiency profile solidified with decades of clinical data, optimizing how vaccines are designed to educate the immune system is becoming increasingly relevant with the emergence of zoonoses and other pathogens. Furthermore, the mRNA vaccine platform would allow for manipulating intracellular machinery involved in antigen processing and

presentation to optimise this process. Antigen processing is surprisingly inefficient in humans, even for high-affinity MHC-I ligands. Strikingly, only 1 in every 10,000 antigens gets presented by MHC-I, leaving a tremendous and somewhat underexplored opportunity for optimization via mRNA vaccine technology [10]. The most relevant aspect of this technology concerning emerging zoonoses is that designing mRNA vaccine constructs generally outpaces the traditional developmental process based on other vaccine platforms, e.g., employing attenuated or inactivated pathogens, due to the availability of software-based tools. It is also less time-consuming than developing subunit protein vaccines, as evidenced during the COVID-19 pandemic and the unseen pace at which mRNA vaccine candidates were manufactured (approx. one month since the whole sequence of SARS-CoV-2 genome was made publicly available).

In line with this, in the present study, we employed many freely available and commercial computational tools to identify and analyze antigenic peptides that belong to the variola virus and MPXV. The most antigenic peptides were incorporated into the conventional mRNA vaccine design, eventuating in a vaccine construct comprised of epitopes stemming from both viruses. The final construct was computationally evaluated for its ability to elicit an immune response, with encouraging predictions regarding antibody production, T cell response longevity, and adequate cytokine production recorded during immune response simulations. Other elements within the construct served as stabilizers, adjuvants, and signalling peptides that should theoretically guide the epitopes into their designated antigen-processing compartments in the context of MHC-I/II. Additional computations were performed regarding stereochemical quality, toxicity, allergenicity, mRNA and mRNA protein product stability, antigenic processing of the construct, as well as its interactions with toll-like receptors (TLRs) and MHC molecules.

Methods

Protein Sequences and Sequence Alignment

Protein sequences of MPXV (strain: Congo 8, accession: KJ642613) and the variola virus

(strain: Isolate Human/India/Ind3/1967, accession: X69198) were retrieved from UniProt. After that, the two proteomes were aligned using the National Center for Biotechnology Information (NCBI) BLASTp algorithm. It was done to identify whether any proteins crucial in pathogenicity or virulence overlap in amino acid sequence to avoid oversaturation of the mRNA construct with genomically identical antigenic elements.

Furthermore, the Pipeline builder for target identification (PBIT) was employed to assess whether the mRNA vaccine protein product shared homology with proteomes belonging to gut microbiome members [11]. Given the emerging body of evidence accumulated in recent years regarding the relevance of the gut microbiome for human homeostasis, vaccines and therapeutics should ideally avoid disrupting the delicate niche in which commensal microorganisms thrive.

CD4+ T Cell Epitope Identification and Selection

Identification of helper T cell (HTL) epitopes was performed using the MHC-II Binding Tool available from the Immune Epitope Database (IEDB) (www.iedb.org). Individual variola and MPXV proteins were screened using the Consensus method, where epitopes with a computed percentile rank ≤ 0.25 were considered for further evaluation [12]. Other computed properties deemed relevant for CD4+ T cell epitope identification included inducibility of TNF, interleukin 4 (IL-4), IL-10 production, allergenicity, and toxicity.

CD8+ T Cell Epitope Identification and Selection

Individual MPXV and variola proteins were screened for cytotoxic T cell (CTL) epitopes using the NetCTL-1.2 server (<https://services.healthtech.dtu.dk/service.php?NetCTL-1.2>) [13]. The approach incorporates predictions for the efficiency of TAP transport, proteasomal C terminal cleavage, and peptide MHC class I binding. The server supports CTL epitope predictions limited to 12 MHC class I supertypes. Artificial neural networks are used to carry out the proteasomal cleavage and MHC class I binding processes. TAP transport efficiency is predicted with a weight matrix. The NetCTL v1.2 server now supports 12 MHC-I supertypes (A1, A2, A3, A24, A26, B7, B8, B27, B39, B44, and B58), all of which were employed in the first screening pro-

cedure, with an epitope identification threshold of 0.75. The IEDB MHC-I immunogenicity tool was then used to test the immunogenicity of each anticipated epitope [14]. Subsequently, the peptides with the highest immunogenicity score were analyzed in terms of MHC binding partners via the IEDB MHC-I binding tool. Peptide sequences with a percentile rank ≤ 2 were considered for further evaluation in the context of allergenicity, toxicity, and probable protective antigenicity.

B Cell Epitopes

The production of long-lasting antibodies that neutralise various virus components hallmarks the immune response to smallpox and, presumably, monkeypox. Ergo, any novel vaccine tailored for these viruses should ensure a humoral immune response of sufficient quality and longevity. In line with this, we screened MPXV and variola virus proteins with antagonistic functions towards the immune response's relevant molecular elements. One such viral protein is the variola virus cytokine response-modifying protein B (Crmb). It binds to host TNF and numerous cytokines, followed by the variola virus B cell lymphoma 2 (Bcl2) homolog F1L, and the MPXV bifunctional 21 KDa precursor protein of 18 KDa membrane fusion protein (B8R). The BepiPred 2.0 server for predicting linear and discontinuous antibody epitopes (<https://services.healthtech.dtu.dk/service.php?BepiPred-2.0>) was used To identify opportunistic linear B cell (LBL) epitopes derived from the variola and MPXV antigenic proteins [15]. The selected LBL epitopes were then screened for allergenicity, toxicity, and antigenicity.

Prediction of Cytokine Inducibility

The ability of the vaccine to elicit cytokine secretion and antigenic response characterizes the vaccine construct's immune response, specifically, the effective stimulation and activation of CD4+. Thus, after antigenicity, toxicity, and allergenicity assessment, the HTL epitopes were screened for the simultaneous response of the cytokines IFN- γ , IL-10, and IL-4 to ensure induction of the adaptive cellular immune response. Therefore, the IL-4Pred [16], IL-10Pred [17], and IFNepitope [18] servers were used to filter the opportunistic HTL epitopes.

Computing Antigenicity, Allergenicity, Toxicity and Physicochemical Properties

Along with the screening of LBL and HTL epitopes, the CTL epitopes initially screened using the IEDB server with an immunogenic score of the 99th percentile were directly screened with the Aller-catPro v2.0 server to predict allergenicity potential [19]. Then, the ToxinPred server was used to predict the toxicity potential of the non-allergenic epitopes by applying the Quantitative Matrix method (mono-peptide) [20]. Finally, the non-toxic and non-allergenic epitopes were screened through the VaxiJen v2.0 server to predict the protective antigen potential of each epitope for subunit vaccine validation using a threshold ≥ 0.5 [21]. Upon completion of the construct design, the antigenicity of the translated open reading frame (ORF) was evaluated using both VaxiJen and ANTIGENpro [22]. The criteria for immunogenic epitope selection rely on them being computed as non-toxic, non-allergenic, and effectually antigenic, screened solely by their physicochemical properties.

The physicochemical properties of the mRNA open reading frame were analysed using the Prot-Param tool in order to compute the overall stability, half-life, and general compositional properties (<https://web.expasy.org/protparam/>) [23]. Prot-Param computes the physicochemical properties from the input protein sequence, independent of performing sequence alignment.

Structure prediction and Molecular Docking

Before performing representative molecular docking simulations between MHC-I/II alleles and their binding partners, binding affinities and bond lengths were computed between each filtered antigenic peptide and their corresponding MHC allele using the Protein-Ligand Interaction Analyzer tool through SAMSON-Connect (OneAngstrom) (<https://www.samson-connect.net>). Then, molecular docking simulations between MHC-I/II alleles and their binding partners were performed using the GalaxyPepDock molecular docking server [24]. MHC-I/II crystal structures were retrieved from the RCSB Protein Data Bank (PDB). If a specific MHC-I/II crystal structure was unavailable, homology modelling was performed using the SWISS-MODEL server. Finally, the sequences were retrieved from the IPD-IMGT/HLA database (<https://www.ebi.ac.uk/ipd/imgt/hla/>). Before molecular docking,

all crystal structures were processed using SAMSON by removing unnecessary ligands, followed by energy minimization through the Swiss-PDB Viewer. Once the 3D structure of the mRNA ORF was predicted using the Phyre2 web server (<http://www.sbg.bio.ic.ac.uk/phyre2/>) for *de novo* protein folding prediction, molecular docking between the mRNA protein product and MHC-I/II and TLR3 was performed using the ClusPro 2.0 protein-protein docking server (<https://cluspro.bu.edu/>) [25]. Docking the protein to MHC-II is particularly relevant, as MHC-II binding is the first step in the cathepsin processing of exogenous antigenic proteins [26]. Before docking the 3D structure of the construct, however, refinement was performed using GalaxyRefine (<https://galaxy.seoklab.org/cgi-bin/submit.cgi?type=REFINE>) [27].

Lastly, the minimum-free energy (MFE) secondary structure of the entire mRNA construct was predicted using the RNAfold web server [28]. The secondary structure of an RNA sequence that contributes the least free energy is the MFE structure. A loop-based energy model and the dynamic programming approach were used to forecast this structure [29]. An RNA secondary structure can be uniquely divided into loops and external bases. Thus the loop-based energy model views the free energy $F(s)$ of an RNA secondary structure s as the total of the contributing free energies FL of the loops L included in s . The secondary structure s that minimizes $F(s)$ is calculated using the selected energy parameter set and the specified temperature (37 °C by default).

Population Coverage Analysis of HLA Variants

The quality of the human immune response to pathogenic microbes and viruses is strongly correlated with the host's immunogenetic constitution. Genetic variants of genes relevant to the immune response determine host susceptibility and allow for either a beneficial or detrimental immunopathologic course to ensue upon infection [30–46]. Among this immune response, genes are those that encode HLA proteins. Polymorphisms within these genes have been strongly correlated with infection outcome and vaccine response. The substantial number of documented HLA variants across different populations suggests that the vaccine design process must factor in HLA variant distribution. Thus, their global distribution was determined once the cor-

responding HLA-I/II alleles were identified during epitope selection. Ensuring that the identified alleles are geographically widely distributed allows the vaccine to protect more individuals. The IEDB Population Coverage Tool was used to compute global allele coverage by factoring in 16 geographical regions [47].

Vaccine Construct Design: Linkers, Trafficking Sequences and Stabilizers

The profiled LBL, HTL, and CTL epitopes, respectively, are part of the open reading frame of the mRNA vaccine construct. The construct upstream and downstream untranslated regions (UTRs), which flank the ORF, generally increase the epitopes' stability, translatability, and adjuvanticity. Moreover, they characterise eukaryotic mRNA. Linkers were used to concatenate the subunits of the 5' UTR, ORF, and 3' UTR for stabilization and have further utility in ensuring that each subunit behaves independently. Furthermore, the linkers are both flexible and rigid enough to allow differentiation between each independent element within the construct.

The N terminus comprises a 7-methylguanosine 5' cap structure and the human β -globin sequence in increasing translational efficiency [48–50]. Correspondingly, the 3' UTR is flanked downstream with the α -globin sequence and a poly(A) tail, respectively, before which a STOP codon is put in place [48]. Additionally, the incorporation of poly(A) tail has been shown to

increase protein expression level with increased length; therefore, the length of the poly(A) tail was extended to 150 residues [48].

The ORF, apart from the epitopes, begins with the Kozak sequence to initiate translation [51]. Following the start codon, a cleavage signal sequence belonging to the tissue plasminogen activator (tPa) was added in order to guide the translational machinery toward product cleavage [52–54]. The tPa sequence is followed by a portion of the human β -defensin protein to increase adjuvanticity (UniProt: A0A7I2-YQ93) [48, 49]. The Signal.P-5.0 web server was employed (<https://services.healthtech.dtu.dk/service.php?SignalP-5.0>) to ensure that the signal sequence would be recognised upon incorporation [55]. As LBLs are located towards the N terminus of the construct, the pan HLA DR-binding epitope (PADRE) sequence was added. Previous work has demonstrated that the incorporating of a PADRE sequence in vaccine designs provides T-cell-aided induction of protective antibodies [56–58]. In order to identify the signal sequence within the tPA protein, the Signal.P-6.0 server was used (Supplementary File 1) [55]. Towards the C terminus, after the final CTL, an AAY-linked MHC Class I trafficking signal domain (MITD) was added in order to guide CTL epitopes toward MHC-I processing (UniProt: Q8WV92) [10]. A schematic representation of the vaccine construct may be found in **Figure 2**.

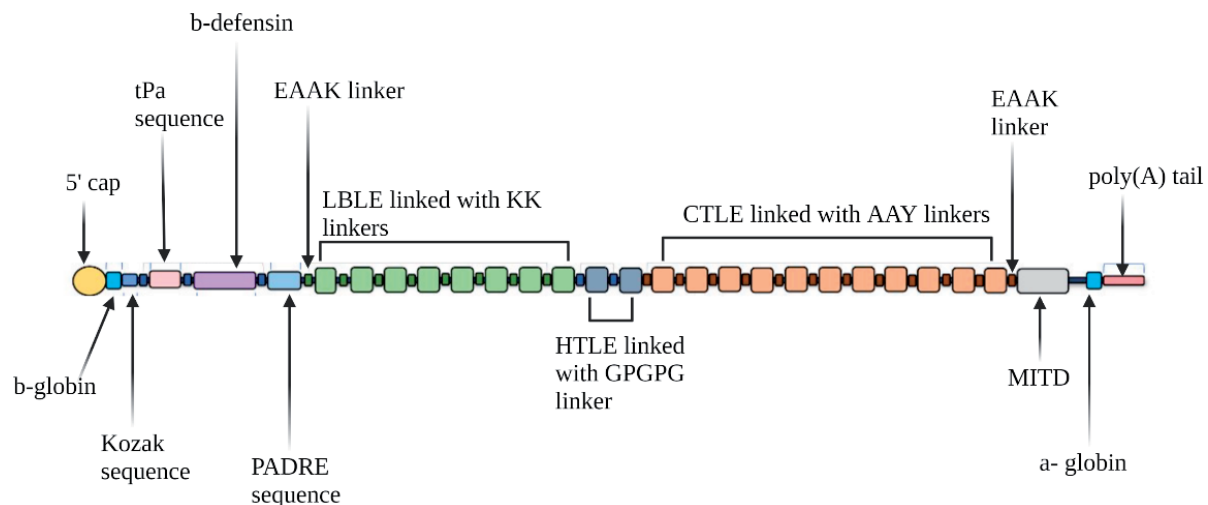


Figure 2. Schematic representation of the mRNA construct design. Abbreviations: tPa – tissue plasminogen activator; LBLE – linear B cell epitopes; HTLE – helper T cell epitopes; CTLE- cytotoxic t cell epitopes; MITD – MHC-I trafficking domain; PADRE – pan HLA DR-binding epitope

Molecular Dynamics Simulations

Upon docking the mRNA vaccine protein product with TLR3, MHC-I, and MHC-II, molecular dynamics (MD) simulations were performed for each complex in order to assess complex stability, using the GROMACS Wizard for SAMSON-Connect [59]. Each complex was placed in a water-containing octahedral box according to the SPC/E water model to achieve this. The boundary was set to at least 10Å from the protein atoms. The addition of Cl⁻ ions performed neutralisation of the solvated structures. The LINCS technique was used to restrict covalent bonds involving hydrogen atoms, while particle-mesh Ewald handled long-range electrostatic interactions using a real-space cutoff of 10Å. In order to eliminate near interactions, the system was first momentarily reduced with the system atoms restricted to the original coordinates (no jumping atoms). The restrained system was then gradually heated to 300 K under constant volume at 0.01ns. Finally, each system was brought into equilibrium for 0.01 ns for NVT and NPT equilibration, using the continuous isothermal-isobaric ensemble at 1 atm and 300 K without constraints. With a 2fs integration time step, the Parrinello-Rahman barostat and a Brendsen thermostat were employed. Production mode for 0.5 ns was applied to run MD simulations, with coordinates recorded every 1000fs. The OPLS-AA/L force field was used for all simulations. mRNA protein product stability was assessed using identical parameters.

Immune System Simulations

The C-Immsim server was employed using the Celada-Seiden model to simulate the vaccine construct humoral and cellular immune response [60, 61]. C-Immsim considers cells as individual agents (agent-based modelling), representing polyclonal models thereof, and quantitatively depicts immune response at the cellular scale. In setting the parameters, the simulation time frame was set to approximately five years (5000-time-steps). Two doses (50 µL simulation volume) were administered, one at time-step 1 and a booster dose at time-step 1095 (one year apart). One advantage of implementing C-Immsim is that an individual simulation may be set up to simulate the immune with user-selected HLA-I/II alleles taken into consideration. In line with this, we

selected HLA alleles that correspondingly to the peptides based on the HLA-I/II epitope screening results, namely *HLA-A02:01*, *HLA-A02:61*, *HLA-B07:02*, *HLA-B39:01*, *HLA-DRB1-07:01*, and *HLA-DRB1-03:01*.

Results

Identification, Evaluation and Selection of T cell and B Cell Epitopes

Considering that the entirety of the available MPXV and variola proteomes underwent screening for potential CTL epitopes, it is not surprising that the initial NetCTL v.1.2. analysis returned thousands of potential CTLs (Supplementary File 1). Only after further computations involving MHC class I immunogenicity and MHC-I binding was further selection possible (Table 1). A similar situation was observed upon initial screening for MHC-II epitopes (see Table 1). Molecular docking results are available in Supplementary File 1.

Corresponding HLA Alleles Are Widely Distributed

The IEDB Population Coverage tool computed a global coverage of 91.33%. In terms of regional coverage, out of the 16 geographical regions included in the computation, all but one (Central America) had a computed coverage score >50% (Figure 2).

The Vaccine Construct: RNA secondary structure, Components, Protein Product and Physicochemical Properties

A total of 23 antigenic peptides were incorporated into the construct; 7 LBL epitopes, 6 HTL epitopes and 10 CTL epitopes. Secondary structure prediction by RNAfold computed a structure whose free thermodynamic ensemble energy is -840.86 kcal/mol (Figure 3). The formulation of the construct is as follows:

5' Cap – human β globin 5' UTR – Kozak context – GPGPG linker – tPa signal sequence – GPGPG linker – human β defensin sequence – GPGPG linker – PADRE sequence – EAAK linker – YSNNEYTPFNK (LBL) – KK linker – CDVGFDSIDI (LBL) – KK linker – TIDSSTIQRRE (LBL) – KK linker – IDDDIDDIDDIDDIDDKASNNDDHN (LBL) – KK linker – NKSTNILDYLSTE (LBL) – KK linker – DISPPDNTIPNISTRE (LBL) – KK linker – YYCLLKSSGCKACVSQTKGIGYGVSGHTSVGDV ICSPCGFTYSHTVSSADKCEPVPNNFTNYIDVEITLYPVNDTSCRTTTTGLSESILTSELTITMNHDCNPVFREEYFVSLNKVATSGFF

Table 1. Summarization of identified cytotoxic, helper T cell and B epitopes, according to VaxiJen score and the most likely HLA variant binders. Peptides with a VaxiJen score ≥ 0.5 were considered potential protective antigens

T Cell Epitopes	VaxiJen Score	HLA Variant
CD4⁺		
KIILISDVRSKRGGN	1.1520	HLA-DRB1*03:01
LDTVNIYISILINHR	0.9376	HLA-DRB1*15:01
VIFYFISISRPKIK	0.8242	HLA-DRB5*01:01
SRLIHFSISFSISLM	1.2229	HLA-DRB1*07:01
RLIHFSISFSISLMQ	1.2158	HLA-DRB1*07:01
MSRLIHFSISFSISL	1.1653	HLA-DRB1*07:01
CD8⁺		
KRRNVEWEL	2.1466	HLA-B*27:05
RGSIIFINY	1.1953	HLA-B*58:01, HLA-B*58:02
FAIIAIVFV	1.3444	HLA-A*02:01, HLA-A*02:06
STIHIIYWGK	1.2641	HLA-A*03:01, HLA-A*26:01
SHVRWRDIW	1.5510	HLA-B*39:01
ATRIEFGPL	2.6960	HLA-B*07:02
NFKIEFEAV	1.8963	HLA-B*08:01
YTNWAILL	1.3359	HLA-A*01:01, HLA-A*02:01, HLA-A*02:06, HLA-A*26:01, HLA-B*39:01, HLA-B*58:01, HLA-B*58:02
KDEAIEIGL	1.6384	HLA-B*44:02, HLA-B*44:03
FKIEFEAVY	1.3717	HLA-A*26:01, HLA-B*27:02, HLA-B*27:05
B Cell Epitopes		
CDVGFDSIDI	1.4667	
IDDIDDIDDIDDIDDIDDKASNNDDHN	1.0407	
DISPPDNTIPNISTRE	0.9703	
TIDSSTIQRRE	0.8453	
YYCLLKGSSGCKACVSTKCGIGYGVSGHTSVGDVICSPCGFGTYSHT-VSSADKCEPVPNNTFNIDVEITLYPVNDTSTRTTTTGLSESILTSELT-ITMNHDCNPVFREEYFVNLNKVATSGFFTGENRYQNISKVCTLNFEIK-CNNKGSFQKLTAKAND	0.7414	
YSNNEYTPFNK	0.6185	
NKSTNILDYLSTE	0.5738	

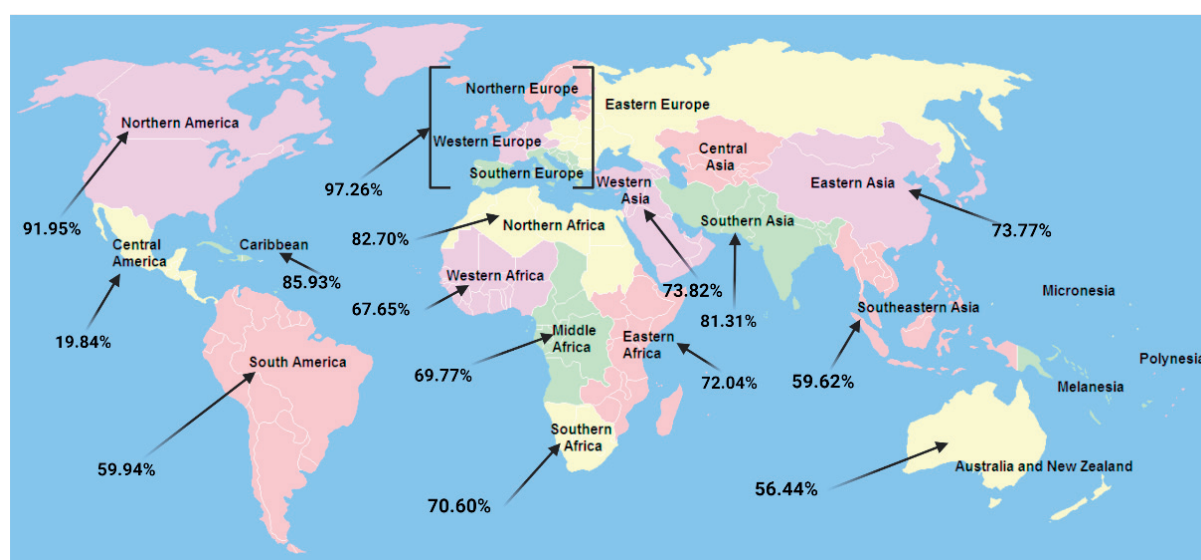


Figure 3. Geographical distribution of HLA allele variants that have been predicted to bind with the identified epitopes

TGENRYQNISKVCTLNFEIKCNKNGSSFKQLTKAKND (LBL) – GPGPG linker – KIILISDVRSKRGGN (HTL) – GPGPG linker – LDTVNIYISILINHR (HTL) – GPGPG linker – VIFYFISIYSRPKIK (HTL) – GPGPG linker – SRLIHFSISFISLSM (HTL) – GPGPG linker – RLIFHSISFISLSMQ (HTL) – GPGPG linker – MSRLIHFSISFISLS (HTL) – AAY linker – KRRNVEWEL (CTL) – AAY linker – RGSIIIFINY (CTL) – AAY linker – FAIIAIVFV (CTL) – AAY linker – STIHIYWGK (CTL) – AAY linker – ATRIEFGPL (CTL) – AAY linker – NFKIEFEAV (CTL) – AAY linker – YTNWAIILL (CTL) – AAY linker – KDEAIEIGL (CTL) – AAY linker – FKIEFEAVY (CTL) – EAAK linker – MIT trafficking signal sequence – GPGPG linker – STOP codon – human α globin 3' UTR – Poly(A) tail.

Toxicity and allergenicity computations estimated that the protein product of the ORF is both non-toxic and non-allergenic, further supplemented with findings of no significant homology between the amino acid sequence of the construct and proteomes belonging to commensal microbes (Supplementary File 1). Physicochemical evaluation of the mRNA protein product computed the protein as stable, with a long-lasting half-life (Table 2). Antigenicity predictions conducted by VaxiJen and ANTIGENpro computed that the mRNA product is a probable protective antigen, with scores of 0.7143 and 0.826646 for VaxiJen and ANTIGENpro, respectively. The Signal.P-6.0 evaluation of the ORF appropriately recognized the incorporated tPa sequence as a signal sequence, indicating a high degree of probability that it will be recognized appropriately during translation (Figure 4).

After the *de novo* protein folding using the Pyhre2 server, the generated PDB structure was

refined using the GalaxyRefine tool, followed by stereochemical evaluation using the Ramachandran plot extension available within the SAMSON-Connect software package. Evaluation of the refined construct returned 90.381% highly preferred observations, followed by 7.463% preferred and 2.156% questionable observations (Figure 5).

The mRNA Product Elicits a Protective and Long-lasting T and B Cell Immune Response

Upon administering the initial dose containing 1000 construct (Ag) units (simulation details in Supplementary File 1), high IgM and, subsequently, IgG antibody titers were documented within the first ten days post-immunization (Figure 6). The observed production of IgG1 corresponds with the predicted solubility-associated computations that classified the protein product as water-soluble, considering that IgG1 is predominantly primed toward hydrophilic antigenic proteins. IgG2 is also simultaneously produced in the primary and secondary immune response. The Ig production as described above corresponds adequately with the observed B cell clonal expansion, where IgM isotype B cells demonstrate high stability across the simulated period, with no tendency to decline. This insight is encouraging, as IgMs are the first responder to foreign organisms and viruses [62]. Though IgG production peaks approximately ten days upon primary and secondary immunization,

Table 2. Summarization of physicochemical, allergenicity, toxicity, and antigenicity properties of the mRNA protein product

Computed Property	Result	Interpretation
Number of amino acids	698	Adequate
Molecular weight	76731.62	Average
Chemical formula	C ₃₄₁₉ H ₅₃₆₄ N ₉₂₂ O ₁₀₂₂ S ₃₁	/
Computed theoretical pI	8.7	Basic
Negatively charged residues (Asp+Glu)	74	/
Positively charged residues (Arg + Lys)	87	/
Number of atoms	10758	/
Instability Index (II)	37.65	Protein is stable
Aliphatic index (AI)	80.82	Protein is thermostable
Grand average of hydropathicity (GRAVY)	-0.256	Protein is hydrophilic
Antigenicity evaluation based on sequence data	0.7143 (VaxiJen)	Construct is predicted as a strong protective antigen
	0.826646 (ANTIGENpro)	
AllerCatPro Evaluation	Probable non-allergen	Protein is a non-allergen
ToxinPred Evaluation	Non-toxin	Protein is non-toxic

A)



B)

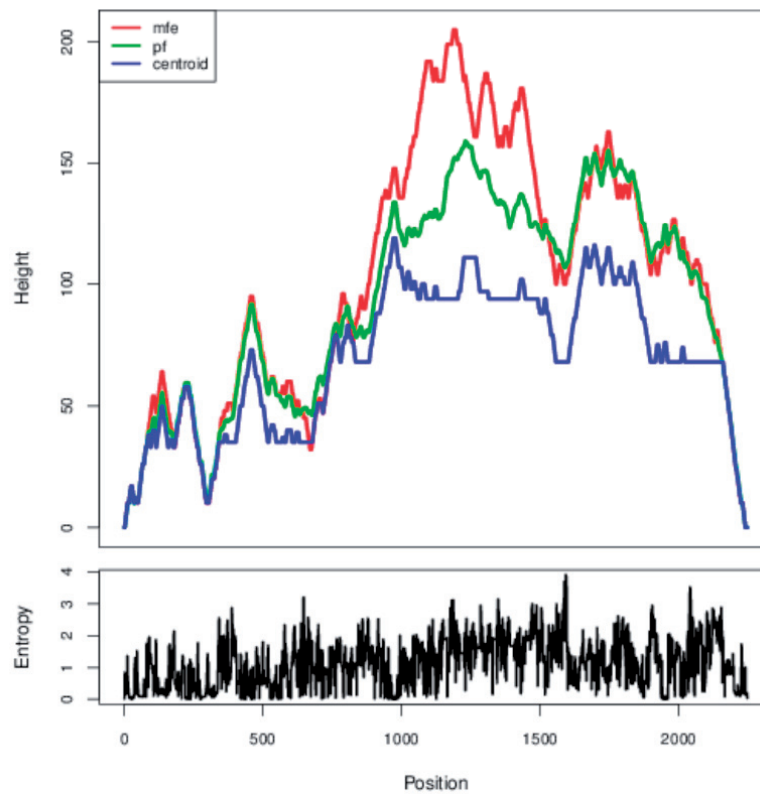


Figure 4. A) RNAfold minimum free energy (MFE) secondary structure prediction of the entire mRNA vaccine construct. B) A mountain plot representation of the MFE structure, the thermodynamic ensemble of RNA structures, and the centroid structure

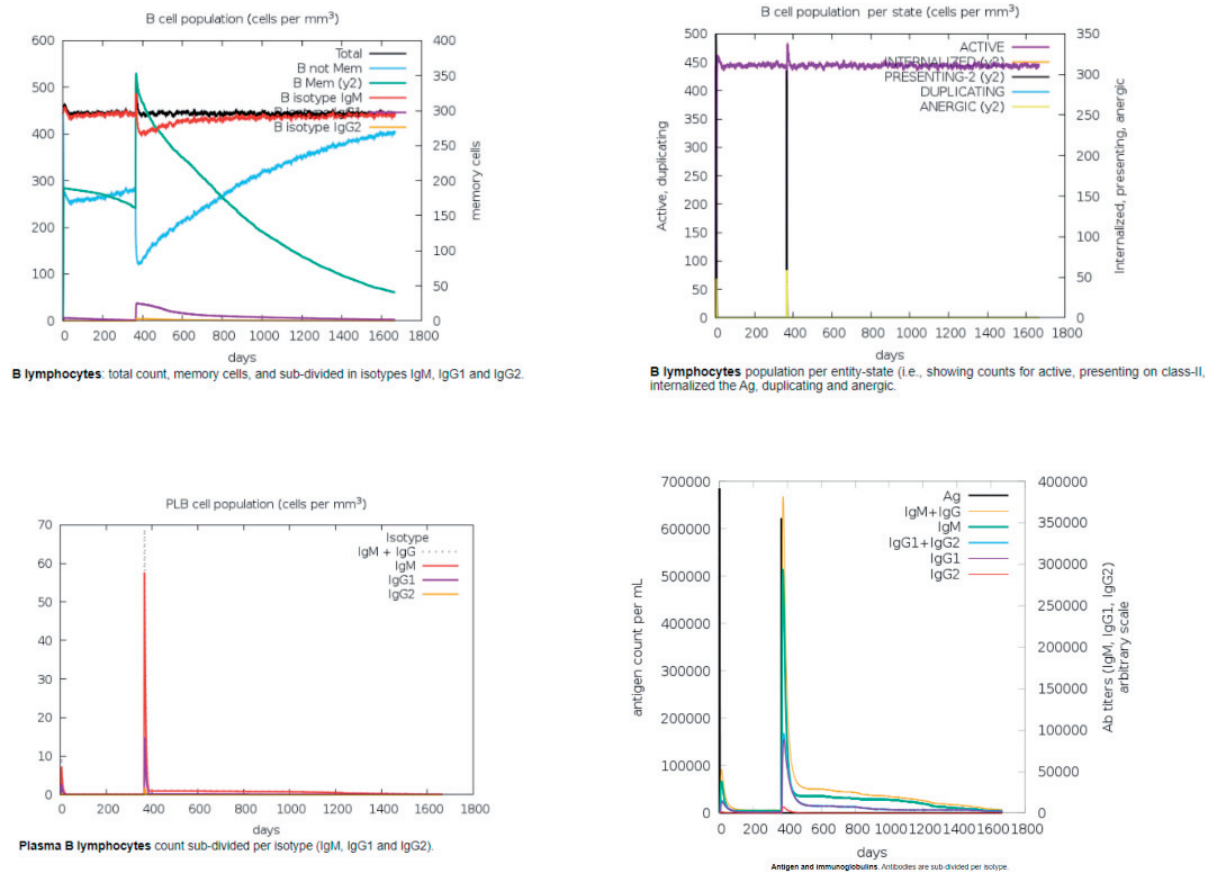


Figure 7. The predicted humoral response to the protein product of the mRNA vaccine construct over five years

differentiated memory HTL pool peaks approximately one month after immunization, followed by a steady decline and subsequent stabilization approximately four years after the second dose. Though active HTLs peak at around day 20 after the initial dose, the amount of active and resting HTLs declines rapidly and stabilises around day 60. Upon the second dose, a robust proliferation of active HTLs is observed, followed by their steady decline and stabilization through conversion towards a resting state some 2.5 years after the second injection. Interestingly, the proliferation of regulatory T cells (Tregs) was significantly more potent after the first dose than the second one. Active and resting Tregs seem to decline significantly and plateau 140 days after the first dose. However, these cells' presence remains consistent despite their minute quantities after the plateau phase. Despite the second dose not offering a significant increase in the resulting repertoire of differentiated Tregs, it maintains detection-worthy counts even five years after the second dose. Perhaps the most encouraging finding is that the immune response to the

vaccine construct is primed towards Th1 immunity, further supported by the predicted cytokine production induced after immunization. The observably high and stable counts of differentiated CD8+ T cells, followed by increased activation in natural killer (NK) cell production and innate immune cell engagement (dendritic cells and macrophages), demonstrated the above.

Molecular Dynamics Simulations

We used GROMACS to simulate the docked complexes (vaccine and TLR-3, MHC-I, and MHC-II) to determine the vaccine-receptor complex's stability. Furthermore, the overall stability of the mRNA protein product was assessed using the same MD parameters. Analyses regarding energy minimization, pressure evaluation, temperature, and estimates of potential energy were carried out. A stable system and a successful MD run were indicated by the simulation system's temperature and pressure during the simulation run and were stable throughout the entire simulation. The overall structural variation of the complex of the

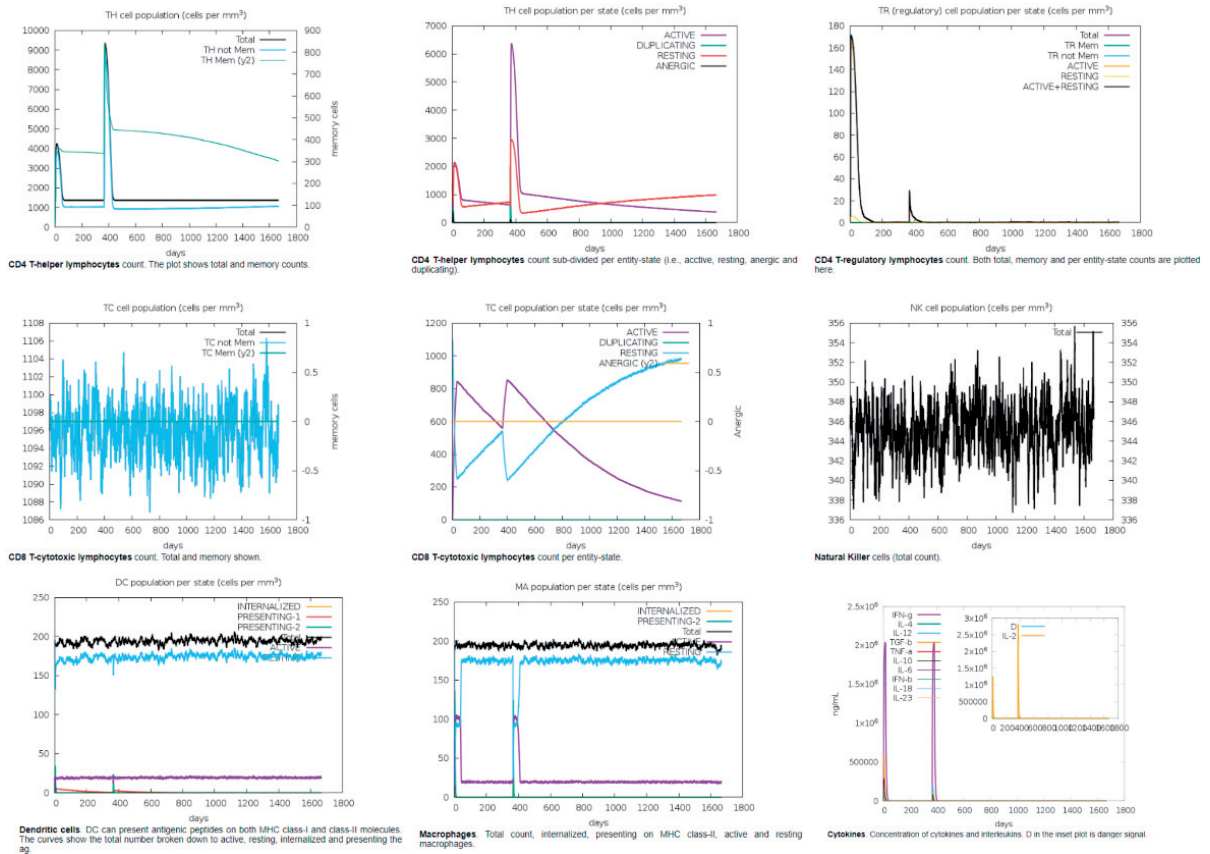


Figure 8. The predicted T cell immune response to the vaccine construct, supplemented with dendritic cell (DC) and macrophage (MA) engagement, supplemented with cytokine secretion profiles

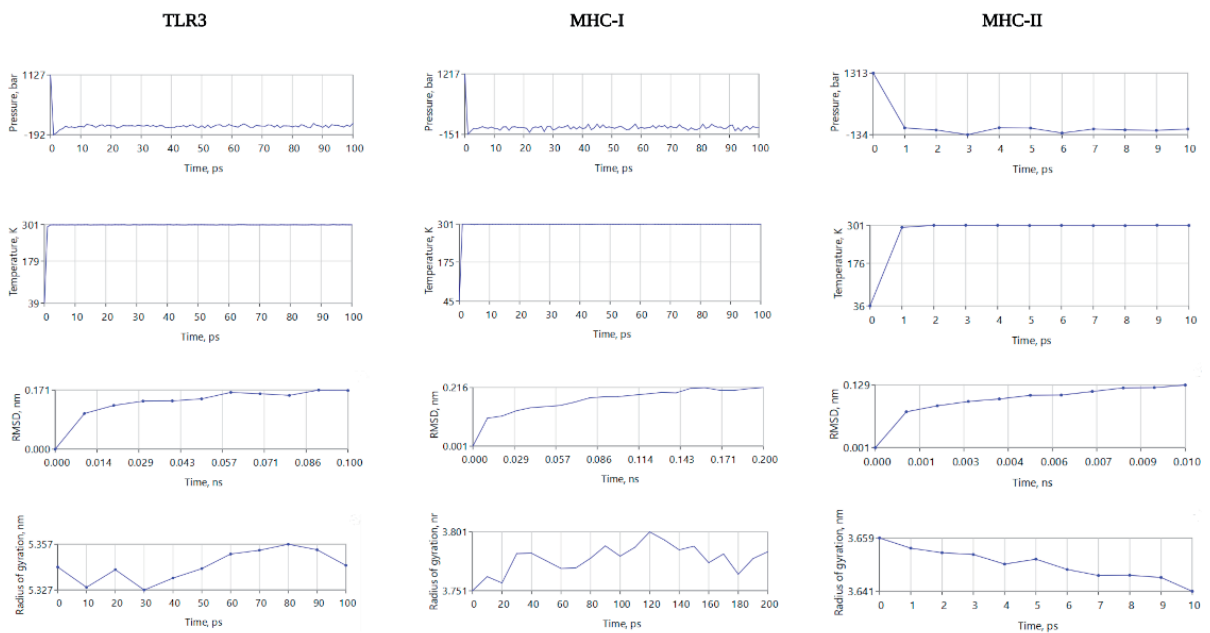


Figure 9. Molecular Dynamics (MD) simulation results for toll-like receptor 3 (TLR3), major histocompatibility complex I (MHC-I), and major histocompatibility complex II (MHC-II) docked with the folded protein product of the vaccine construct. The image displays results in the context of system pressure, temperature, and root mean square deviation (RMSD) of the docked complexes, along with the gyration radius

vaccine and immune receptor is depicted by the complex root mean square deviation (RMSD) (See **Figure 8, A**). The protein product alone has also been computed as stable when simulated under the same MD production run parameters (see Supplementary File 1).

Discussion

Though human smallpox was eradicated from the human population in the 1980s, the notion that an intentional variola virus release may occur has helped maintain the relevance of studying human orthopoxviruses. With this in mind, it is not all surprising that the majority of smallpox-related data stems from research conducted on the human Vaccinia virus rather than variola, as variola is classified as a level 4 biological agent stored in only a small number of laboratories. On the other hand, the recent outbreak of MPXV gave rise to a rather indicative body of research regarding the virus's genomics, proteomics and host-pathogen immunobiology, which may be opportunistically used for better understanding of variola as well. A very useful body of immunological data pertaining to T cell and B cell immunity is therefore available. An opportunity lies in merging these insights with computational tools to more accurately understand MPXV and variola, particularly with vaccine design. Though much remains to be uncovered, the currently-available data on MPXV infection offers clues into what sort of protective immune response profile should be elicited by a novel vaccine.

During severe MPXV infection, the cytokine profile suggests a dominant Th2 response associated with cytokine storm development [64]. Th2 cytokines (IL-10, IL-4, IL-13, IL-5, IL-6) are elevated during clinically severe infections, of which IL-10 and IL-4 dampen Th1 response [64], [65]. IL-10 downregulates Th1 cytokines (IL-2, TNF- α , IL-12, IFN- γ), indicating the cytokine storm's onset. Our immune response simulation results display a favourable, Th1-orientated response upon vaccination, suggesting T regulatory cell response and prolonged B cell and effector T cell survival. The process is further supplemented with the vaccine-induced cytokine secretion profile recorded within this work, indicating an IFN-mediated immune response. During the innate

immune response against MPXV, it has been observed that the impairment in NK cells causes the dysregulation of IFN- γ and TNF- α secretion [4, 5, 64–66]. Though monocytes play a critical role in shaping the adaptive immune response, subsequent cytokine release that induces monocyte cytotoxicity for viral dissemination is insufficient in countering cytokine storm-induced toxemia [67]. Moreover, the inability to induce an effective IFN response was associated with disease severity; adaptive immune response in eradicating virus-infected monocytes via IFN- γ secreting CD8+ cells was proven for sufficient protection, independent of CD4+ and B cells [68]. Considering our implementation of LBL epitopes, the incorporation of the apoptosis inhibitor F1L, IFN- γ binding proteins B8R, and the TNF and chemokine binding protein CrmB may effectively encompass the specific viral evasion strategies to host immune response in both intrinsic and extrinsic pathways for leveraging secreted antibodies [69–71]. Thus, the inclusion of characterized B cell epitopes and systematically defined HTL and CTL epitopes help accurately profile MPXV infection. This beneficial immunological response was recorded for our vaccine design, suggesting that the vaccine would most likely offer sufficient protection within this context. Following stimulation of T cells and subsequent antibody development, B cells and antibody production have notably indicated that protective IgG+ memory B cells highlight protection alone [67]. While this insight warrants further investigation in a population-specific context, it is encouraging that our vaccine design elicits IgG+-specific B cell production, along with stable and long-lasting IgG antibody titers. Overall, the predicted immunological response to the protein product of the vaccine construct would theoretically induce a beneficial Th1-mediated protective immune response. Stimulation of Th1 immunity is also a key protective factor against variola [4–6, 72]. With this in mind, the proposed vaccine design may protect against human smallpox, considering that the immune response simulation results satisfy the necessary criteria that hallmark protective immunity against the virus. The above is not surprising considering the genomic and host-pathogen similarities between variola and MPXV. An attractive hypothesis that may be drawn from this work is that this vaccine would offer cross-protection against other orthopox-

viruses, considering the number of diverse antigens incorporated into the construct.

Safety and antigenicity computations have classified the mRNA protein product as a non-allergenic, non-toxic, and highly-antigenic protein with no significant homology with the human gut microbiota. In terms of homology between human-derived signalling and trafficking elements incorporated within the construct, homology prediction was not performed, as these sequences are expected to be cleaved during translation.

Despite the encouraging results obtained from this study, its limitations should be adequately addressed. Namely, whilst epitope identification using the IEDB analysis toolkit has been broadly used for theoretical vaccine design in the past, their accuracy entirely relies on the quality of the datasets used to train the implemented algorithms. However, IEDB still stands as an acceptable tool for epitope identification. MHC-I processing prediction, on the other hand, is a complex and inefficient system, leaving room for algorithm improvement and forming the need for experimental validation in terms of antigenic processing. Furthermore, computational tools currently need to be available to predict the interaction between the host's cellular machinery and an introduced exogenous mRNA construct in a reliable fashion. Thus, all of our simulation results stem from analyzing the specific protein product encoded by the mRNA ORF rather than considering the process of mRNA translation or validating whether the translational machinery will recognize the cleavage/trafficking sequences *in vivo*. To compensate for this shortcoming, we employed SignalP-5.0, which detects the presence of signal sequences based on a protein's amino acid code. The tPA signal sequence was adequately detected upon incorporation within the construct, allowing us to hypothesize that the translational machinery would most likely recognize its presence. However, the major drawback of this study is the lack of *in vivo* data regarding our vaccine design, coupled with the fact that there are no computational tools for evaluating mRNA vaccines on a cellular level. Analyses of the protein product revealed encouraging results, even when the various partitions of the mRNA construct would not be guided by replication machinery towards different antigen processing compart-

ments (MHC-I/II). All this was revealed through molecular docking and subsequent molecular dynamics simulations between the mRNA product complexed with MHC-I/II and TLR3. Furthermore, the C-Immsim server, although the gold standard for open-source *in silico* immune response predictions, does not take into account the delivery method used and suffers from the inability for a greater number of HLA alleles to be specified within the input parameters. Additionally, the degree to which the statement of quantity is near that quantity's actual (true) value is known as the forecast's accuracy. Because the forecast is a statement about the future, the actual value is typically impossible to measure when issued, which should be considered when interpreting results from such forecasting tools. In line with this, another C-Immsim simulation was carried out for one year, with the second dose being omitted (Supplementary File 1). Considering that TLR3 can detect virus-associated nucleic acid and peptide sequences, a molecular dynamics simulation was performed on the docked mRNA-TLR3 complex in order to determine the stability of this complex. Furthermore, the overall stability of the mRNA protein product was further assessed using MD simulations. Though MD simulations and molecular docking have drawbacks regarding the accuracy and *in vitro* and *in vivo* translatability, they still represent well-accepted methods for *in silico* biophysical analysis of large molecular structures.

Overall, this work describes a novel conventional mRNA-based vaccine design, which incorporates various potential antigenic targets stemming from the variola virus and MPXV, in an attempt to design a vaccine that would elicit a protective immune response against these and other orthopoxviruses. In the confines of *in silico* evaluation, the vaccine design satisfies all safety, antigenicity and immune response longevity criteria. Furthermore, according to previous works, the Th1-oriented immune response elicited by the vaccine would offer sufficient protection against both viruses. Choosing the mRNA vaccine platform stems from the added potential of increasing antigen presentation to increase vaccine efficiency, safety and design speed. Yet the specific relationship between the mRNA construct and the intracellular machinery warrants *in vivo* validation. Taken altogether, our work elegantly dem-

onstrates the immense potential that computational tools hold for fast and relatively accurate streamlining of vaccine design, as this approach may be extrapolated to peptide-based and protein subunit vaccines.

Lastly, in terms of biosafety aspects, this design and pipeline represent a potentially fruitful avenue to pursue. They allow the rapid development of protective vaccines based on genomic or proteomic data. Furthermore, due to the opportunity to enhance antigen processing via the incorporation of trafficking and signal domains and predict various potential biophysical and immunological outcomes, this technology may be a valuable tool in the case of biological threats.

Acknowledgements

Supplementary Materials: All supplementary materials from Supplementary File 1 can be found on the following link: <https://doi.org/10.5281/zenodo.7264789>

Author Contributions: Conceptualization, Dženan Kovačić; methodology, Dženan Kovačić.; software, Dženan Kovačić.; validation, Dženan Kovačić; formal analysis, Dženan Kovačić and Adna Salihović; investigation, Dženan Kovačić and Adna Salihović; resources, Dženan Kovačić and Adna Salihović; data curation, Dženan Kovačić.; writing—original draft preparation, Dženan Kovačić.; writing—review and editing, Adna Salihović and Dženan Kovačić.; visualization, Dženan Kovačić and Adna Salihović; supervision, Dženan Kovačić.; project administration, Dženan Kovačić. All authors have read and agreed to the published version of the manuscript.

Data Availability Statement: The epitope screening and identification data are freely available from public repositories, with sequence and proteome names clearly stated within the manuscript. All other data generated through commercial software is available within the Supplementary Files.

Acknowledgements: We appreciate professors Andrej A. Gajić, Riad Hajdarević, PhD, and Damir Marjanović, PhD, for their continuous support during the conceptualisation and preparation of this manuscript.

Conflict of interest statement

The authors declare no conflict of interest.

Funding sources

There are no sources of funding to declare.

References

1. G. McFadden, "Poxvirus tropism," *Nature Reviews Microbiology* 2005 3:3, vol. 3, no. 3, pp. 201–213, Mar. 2005, doi: 10.1038/nrmicro1099. DOI: <https://doi.org/10.1038/nrmicro1099>

2. V. Panchanathan, G. Chaudhri, and G. Karupiah, "Protective Immunity against Secondary Poxvirus Infection Is Dependent on Antibody but Not on CD4 or CD8 T-Cell Function," *J Virol*, vol. 80, no. 13, pp. 6333–6338, Jul. 2006, DOI: 10.1128/JVI.00115-06/ASSET/6028F5A2-E462-4916-9DFD-D56048F-D574A/ASSETS/GRAPHIC/ZJV0130679310006. JPEG. DOI: <https://doi.org/10.1128/JVI.00115-06>
3. E. Hammarlund, A. Dasgupta, C. Pinilla, P. Norori, K. Früh, and M. K. Slifka, "Monkeypox virus evades antiviral CD4+ and CD8+ T cell responses by suppressing cognate T cell activation," *Proc Natl Acad Sci U S A*, vol. 105, no. 38, pp. 14567–14572, Sep. 2008, DOI: 10.1073/PNAS.0800589105/SUPPL_FILE/0800589105SI.PDF. DOI: <https://doi.org/10.1073/pnas.0800589105>
4. R. B. Kennedy, I. G. Ovsyannikova, R. M. Jacobson, and G. A. Poland, "The immunology of smallpox vaccines," *Curr Opin Immunol*, vol. 21, no. 3, p. 314, Jun. 2009, DOI: 10.1016/J.COI.2009.04.004. DOI: <https://doi.org/10.1016/j.coi.2009.04.004>
5. I. J. Amanna, M. K. Slifka, and S. Crotty, "Immunity and immunological memory following smallpox vaccination," *Immunol Rev*, vol. 211, no. 1, pp. 320–337, Jun. 2006, DOI: 10.1111/J.0105-2896.2006.00392.X. DOI: <https://doi.org/10.1111/j.0105-2896.2006.00392.x>
6. E. Hammarlund et al., "Duration of antiviral immunity after smallpox vaccination," *Nat Med*, vol. 9, no. 9, pp. 1131–1137, Sep. 2003, DOI: 10.1038/NM917. DOI: <https://doi.org/10.1038/nm917>
7. J. Stabenow, R. M. Buller, J. Schriewer, C. West, J. E. Sagartz, and S. Parker, "A Mouse Model of Lethal Infection for Evaluating Prophylactics and Therapeutics against Monkeypox Virus," *J Virol*, vol. 84, no. 8, p. 3909, Apr. 2010, DOI: 10.1128/JVI.02012-09. DOI: <https://doi.org/10.1128/JVI.02012-09>
8. W. D. Arndt et al., "Evasion of the Innate Immune Type I Interferon System by Monkeypox Virus," *J Virol*, vol. 89, no. 20, pp. 10489–10499, Oct. 2015, DOI: 10.1128/JVI.00304-15/ASSET/A137DDCD-D53E-4875-8349-F21F04AB867D/ASSETS/GRAPHIC/ZJV9990908700008.JPEG. DOI: <https://doi.org/10.1128/JVI.00304-15>
9. H. Yu, R. C. Bruneau, G. Brennan, and S. Rothenburg, "Battle Royale: Innate Recognition of Poxviruses and Viral Immune Evasion," *Biomedicines* 2021, Vol. 9, Page 765, vol. 9, no. 7, p. 765, Jul. 2021, DOI: 10.3390/BIOMEDICINES9070765. DOI: <https://doi.org/10.3390/biomedicines9070765>
10. S. Kreiter et al., "Increased Antigen Presentation Efficiency by Coupling Antigens to MHC Class I Trafficking Signals," *The Journal of Immunology*, vol. 180, no. 1, pp. 309–318, Jan. 2008, DOI: 10.4049/JIMMUNOL.180.1.309. DOI: <https://doi.org/10.4049/jimmunol.180.1.309>
11. G. Shende et al., "PBIT: Pipeline Builder for Identification of drug Targets for infectious diseases," *Bioinformatics*, vol. 33, no. 6, pp. 929–931, Mar. 2017, DOI: 10.1093/BIOINFORMATICS/BTW760. DOI: <https://doi.org/10.1093/bioinformatics/btw760>
12. P. Wang et al., "Peptide binding predictions for HLA DR, DP and DQ molecules," *BMC Bioinformatics*, vol.

- 11, p. 568, Nov. 2010, DOI: 10.1186/1471-2105-11-568. DOI: <https://doi.org/10.1186/1471-2105-11-568>
13. M. v. Larsen, C. Lundegaard, K. Lamberth, S. Buus, O. Lund, and M. Nielsen, "Large-scale validation of methods for cytotoxic T-lymphocyte epitope prediction," *BMC Bioinformatics*, vol. 8, no. 1, pp. 1–12, Oct. 2007, DOI: 10.1186/1471-2105-8-424/TABLES/3. DOI: <https://doi.org/10.1186/1471-2105-8-424>
 14. J. J. A. Calis et al., "Properties of MHC Class I Presented Peptides That Enhance Immunogenicity", *PLoS Comput Biol*, vol. 9, no. 10, p. 1003266, 2013, DOI: 10.1371/JOURNAL.PCBI.1003266. DOI: <https://doi.org/10.1371/journal.pcbi.1003266>
 15. M. C. Jespersen, B. Peters, M. Nielsen, and P. Marcantili, "BepiPred-2.0: improving sequence-based B-cell epitope prediction using conformational epitopes," *Nucleic Acids Res*, vol. 45, no. Web Server issue, p. W24, Jul. 2017, DOI: 10.1093/NAR/GKX346. DOI: <https://doi.org/10.1093/nar/gkx346>
 16. S. K. Dhanda, S. Gupta, P. Vir, and G. P. Raghava, "Prediction of IL4 inducing peptides.," *Clin Dev Immunol*, vol. 2013, p. 263952, 2013, DOI: 10.1155/2013/263952. DOI: <https://doi.org/10.1155/2013/263952>
 17. G. Nagpal et al., "Computer-aided designing of immunosuppressive peptides based on IL-10 inducing potential," *Sci Rep*, vol. 7, Feb. 2017, DOI: 10.1038/SREP42851. DOI: <https://doi.org/10.1038/srep42851>
 18. S. K. Dhanda, P. Vir, and G. P. S. Raghava, "Designing of interferon-gamma inducing MHC class-II binders," *Biol Direct*, vol. 8, no. 1, p. 30, Dec. 2013, DOI: 10.1186/1745-6150-8-30. DOI: <https://doi.org/10.1186/1745-6150-8-30>
 19. M. N. Nguyen, N. L. Krutz, V. Limviphuvadh, A. L. Lopata, G. F. Gerberick, and S. Maurer-Stroh, "AllerCatPro 2.0: a web server for predicting protein allergenicity potential," *Nucleic Acids Res*, no. 1, May 2022, DOI: 10.1093/NAR/GKAC446. DOI: <https://doi.org/10.1093/nar/gkac446>
 20. N. Sharma, L. D. Naorem, S. Jain, and G. P. S. Raghava, "ToxinPred2: an improved method for predicting toxicity of proteins," *Brief Bioinform*, May 2022, DOI: 10.1093/BIB/BBAC174. DOI: <https://doi.org/10.1093/bib/bbac174>
 21. I. A. Doytchinova and D. R. Flower, "VaxiJen: A server for prediction of protective antigens, tumour antigens and subunit vaccines," *BMC Bioinformatics*, vol. 8, no. 1, pp. 1–7, Jan. 2007, DOI: 10.1186/1471-2105-8-4/TABLES/2. DOI: <https://doi.org/10.1186/1471-2105-8-4>
 22. C. N. Magnan et al., "High-throughput prediction of protein antigenicity using protein microarray data," *Bioinformatics*, vol. 26, no. 23, p. 2936, Dec. 2010, DOI: 10.1093/BIOINFORMATICS/BTQ551. DOI: <https://doi.org/10.1093/bioinformatics/btq551>
 23. E. Gasteiger et al., "Protein Identification and Analysis Tools on the ExPASy Server," *The Proteomics Protocols Handbook*, pp. 571–607, 2005, DOI: 10.1385/1-59259-890-0:571. DOI: <https://doi.org/10.1385/1-59259-890-0:571>
 24. H. Lee, L. Heo, M. S. Lee, and C. Seok, "GalaxyPepDock: A protein-peptide docking tool based on interaction similarity and energy optimization," *Nucleic Acids Res*, vol. 43, no. W1, pp. W431–W435, 2015, DOI: 10.1093/nar/gkv495. DOI: <https://doi.org/10.1093/nar/gkv495>
 25. L. A. Kelley, S. Mezulis, C. M. Yates, M. N. Wass, and M. J. E. Sternberg, "The Phyre2 web portal for protein modelling, prediction and analysis," *Nat Protoc*, vol. 10, no. 6, p. 845, Jun. 2015, DOI: 10.1038/NPROT.2015.053. DOI: <https://doi.org/10.1038/nprot.2015.053>
 26. S. Sadegh-Nasseri and A. R. Kim, "Exogenous Antigens Bind MHC Class II first, and Are Processed by Cathepsins Later," *Mol Immunol*, vol. 68, no. 2 0 0, p. 81, Jul. 2015, DOI: 10.1016/J.MOLIMM.2015.07.018. DOI: <https://doi.org/10.1016/j.molimm.2015.07.018>
 27. J. Ko, H. Park, L. Heo, and C. Seok, "GalaxyWEB server for protein structure prediction and refinement," *Nucleic Acids Res*, vol. 40, no. Web Server issue, p. W294, Jul. 2012, DOI: 10.1093/NAR/GKS493. DOI: <https://doi.org/10.1093/nar/gks493>
 28. R. Lorenz et al., "ViennaRNA Package 2.0," *Algorithms for Molecular Biology*, vol. 6, no. 1, pp. 1–14, Nov. 2011, DOI: 10.1186/1748-7188-6-26/TABLES/2. DOI: <https://doi.org/10.1186/1748-7188-6-26>
 29. I. L. Hofacker and P. F. Stadler, "Memory efficient folding algorithms for circular RNA secondary structures," *Bioinformatics*, vol. 22, no. 10, pp. 1172–1176, May 2006, DOI: 10.1093/BIOINFORMATICS/BTL023. DOI: <https://doi.org/10.1093/bioinformatics/btl023>
 30. J. R. Delanghe, M. M. Speeckaert, and M. L. de Buyzere, "COVID-19 infections are also affected by human ACE1 D/I polymorphism.," *Clin Chem Lab Med*, Apr. 2020, DOI: 10.1515/cclm-2020-0425. DOI: <https://doi.org/10.1515/cclm-2020-0425>
 31. S. Itoyama et al., "ACE1 polymorphism and progression of SARS," *Biochem Biophys Res Commun*, vol. 323, no. 3, pp. 1124–1129, Oct. 2004, DOI: 10.1016/j.bbrc.2004.08.208. DOI: <https://doi.org/10.1016/j.bbrc.2004.08.208>
 32. M. Harishankar, P. Selvaraj, and R. Bethunaickan, "Influence of genetic polymorphism towards pulmonary tuberculosis susceptibility," *Front Med (Lausanne)*, vol. 5, no. AUG, pp. 1–1, 2018, DOI: 10.3389/fmed.2018.00213. DOI: <https://doi.org/10.3389/fmed.2018.00213>
 33. S. Anooosheh, P. Farnia, and M. Kargar, "Association between TNF-Alpha (-857) Gene Polymorphism and Susceptibility to Tuberculosis," 2011.
 34. M. W. Ng et al., "The association of RANTES polymorphism with severe acute respiratory syndrome in Hong Kong and Beijing Chinese," *BMC Infect Dis*, vol. 7, no. 1, pp. 1–8, Jun. 2007, DOI 10.1186/1471-2334-7-50. DOI: <https://doi.org/10.1186/1471-2334-7-50>
 35. H. B. Oral et al., "Interleukin-10 (IL-10) gene polymorphism as a potential host susceptibility factor in tuberculosis," *Cytokine*, vol. 35, no. 3–4, pp. 143–147, Aug. 2006, DOI: 10.1016/j.cyto.2006.07.015. DOI: <https://doi.org/10.1016/j.cyto.2006.07.015>
 36. P. Selvaraj, K. Alagarasu, M. Harishankar, M. Vidyarani, D. Nisha Rajeswari, and P. R. Narayanan, "Cytokine gene polymorphisms and cytokine levels in pulmonary tuberculosis," *Cytokine*, vol. 43, no. 1, pp. 26–33,

- Jul. 2008, DOI: 10.1016/j.cyto.2008.04.011. DOI: <https://doi.org/10.1016/j.cyto.2008.04.011>
37. K. Y. K. Chan et al., "CD209 (DC-SIGN) -336A>G promoter polymorphism and severe acute respiratory syndrome in Hong Kong Chinese," *Hum Immunol*, vol. 71, no. 7, pp. 702–707, Jul. 2010, DOI: 10.1016/j.humimm.2010.03.006. DOI: <https://doi.org/10.1016/j.humimm.2010.03.006>
 38. Y. X. Yi, J. B. Han, L. Zhao, Y. Fang, Y. F. Zhang, and G. Y. Zhou, "Tumor necrosis factor alpha gene polymorphism contributes to pulmonary tuberculosis susceptibility: Evidence from a meta-analysis," *Int J Clin Exp Med*, vol. 8, no. 11, pp. 20690–20700, Nov. 2015.
 39. M. Akahoshi et al., "Influence of interleukin-12 receptor β 1 polymorphisms on tuberculosis," *Hum Genet*, vol. 112, no. 3, pp. 237–243, Mar. 2003, DOI: 10.1007/s00439-002-0873-5. DOI: <https://doi.org/10.1007/s00439-002-0873-5>
 40. L. Ka, M. Hospital, S. T. Lai, K. M. So, and U.-S. Khoo, "Association of a single nucleotide polymorphism in the CD209 (DC-SIGN) promoter with SARS severity Key Messages," *Hong Kong Med J*, vol. 16, no. 5, p. 37, 2010.
 41. F. F. Yuan et al., "Influence of Fc γ RIIA and MBL polymorphisms on severe acute respiratory syndrome," *Tissue Antigens*, vol. 66, no. 4, pp. 291–296, Oct. 2005, DOI: 10.1111/j.1399-0039.2005.00476.x. DOI: <https://doi.org/10.1111/j.1399-0039.2005.00476.x>
 42. N. Remus et al., "Association of IL12RB1 Polymorphisms with Pulmonary Tuberculosis in Adults in Morocco," *J Infect Dis*, vol. 190, no. 3, pp. 580–587, Aug. 2004, DOI: 10.1086/422534. DOI: <https://doi.org/10.1086/422534>
 43. M. Bukhari et al., "TLR8 gene polymorphism and association in bacterial load in southern Punjab of Pakistan: An association study with pulmonary tuberculosis," *Int J Immunogenet*, vol. 42, no. 1, pp. 46–51, Feb. 2015, DOI: 10.1111/iji.12170. DOI: <https://doi.org/10.1111/iji.12170>
 44. S. P. Anand, P. Selvaraj, M. S. Jawahar, A. R. Adhilakshmi, and P. R. Narayanan, "Interleukin-12B & interleukin-10 gene polymorphisms in pulmonary tuberculosis," *Indian Journal of Medical Research*, vol. 126, no. 2, pp. 135–138, Aug. 2007.
 45. K. M. Adam, "Immunoinformatics approach for multi-epitope vaccine design against structural proteins and ORF1a polyprotein of severe acute respiratory syndrome coronavirus-2 (SARS-CoV-2)," *Trop Dis Travel Med Vaccines*, vol. 7, no. 1, pp. 1–13, Dec. 2021, DOI: 10.1186/s40794-021-00147-1/FIGURES/7. DOI: <https://doi.org/10.1186/s40794-021-00147-1>
 46. R. Monteiro-Maia, M. B. Ortigão-de-Sampaio, R. T. Pinho, and L. R. R. Castello-Branco, "Modulation of humoral immune response to oral BCG vaccination by *Mycobacterium bovis* BCG Moreau Rio de Janeiro (RDJ) in healthy adults," *J Immune Based Ther Vaccines*, vol. 4, no. 1, pp. 1–6, Sep. 2006, DOI: 10.1186/1476-8518-4-4/FIGURES/4. DOI: <https://doi.org/10.1186/1476-8518-4-4>
 47. H. H. Bui, J. Sidney, K. Dinh, S. Southwood, M. J. Newman, and A. Sette, "Predicting population coverage of T-cell epitope-based diagnostics and vaccines," *BMC Bioinformatics*, vol. 7, p. 153, Mar. 2006, doi: 10.1186/1471-2105-7-153. DOI: <https://doi.org/10.1186/1471-2105-7-153>
 48. T. Schlake, A. Thess, M. Fotin-Mleczek, and K. J. Kallen, "Developing mRNA-vaccine technologies," *RNA Biol*, vol. 9, no. 11, p. 1319, 2012, DOI: 10.4161/RNA.22269. DOI: <https://doi.org/10.4161/rna.22269>
 49. N. Pardi, M. J. Hogan, F. W. Porter, and D. Weissman, "mRNA vaccines – a new era in vaccinology," *Nature Reviews Drug Discovery* 2018 17:4, vol. 17, no. 4, pp. 261–279, Jan. 2018, DOI: 10.1038/nrd.2017.243. DOI: <https://doi.org/10.1038/nrd.2017.243>
 50. I. Ahammad and S. S. Lira, "Designing a novel mRNA vaccine against SARS-CoV-2: An immunoinformatics approach," *Int J Biol Macromol*, vol. 162, pp. 820–837, Nov. 2020, DOI: 10.1016/j.ijbiomac.2020.06.213. DOI: <https://doi.org/10.1016/j.ijbiomac.2020.06.213>
 51. M. Kozak, "Possible role of flanking nucleotides in recognition of the AUG initiator codon by eukaryotic ribosomes," *Nucleic Acids Res*, vol. 9, no. 20, pp. 5233–5252, Oct. 1981, DOI: 10.1093/NAR/9.20.5233. DOI: <https://doi.org/10.1093/nar/9.20.5233>
 52. J. Y. Wang et al., "Improved expression of secretory and trimeric proteins in mammalian cells via the introduction of a new trimer motif and a mutant of the tPA signal sequence," *Appl Microbiol Biotechnol*, vol. 91, no. 3, pp. 731–740, Aug. 2011, DOI: 10.1007/S00253-011-3297-0/FIGURES/6. DOI: <https://doi.org/10.1007/s00253-011-3297-0>
 53. C. Seillier et al., "Roles of the tissue-type plasminogen activator in immune response," *Cell Immunol*, vol. 371, p. 104451, Jan. 2022, DOI: 10.1016/J.CELLIMM.2021.104451. DOI: <https://doi.org/10.1016/j.cellimm.2021.104451>
 54. Y. Kou et al., "Tissue plasminogen activator (tPA) signal sequence enhances immunogenicity of MVA-based vaccine against tuberculosis," *Immunol Lett*, vol. 190, pp. 51–57, Oct. 2017, DOI: 10.1016/J.IMLET.2017.07.007. DOI: <https://doi.org/10.1016/j.imlet.2017.07.007>
 55. F. Teufel et al., "SignalP 6.0 predicts all five types of signal peptides using protein language models," *Nature Biotechnology* 2022 40:7, vol. 40, no. 7, pp. 1023–1025, Jan. 2022, DOI: 10.1038/s41587-021-01156-3. DOI: <https://doi.org/10.1038/s41587-021-01156-3>
 56. E. D. Franke et al., "Pan DR binding sequence provides T-cell help for induction of protective antibodies against *Plasmodium yoelii* sporozoites," *Vaccine*, vol. 17, no. 9–10, pp. 1201–1205, Mar. 1999, DOI: 10.1016/S0264-410X(98)00341-7. DOI: [https://doi.org/10.1016/S0264-410X\(98\)00341-7](https://doi.org/10.1016/S0264-410X(98)00341-7)
 57. J. Alexander et al., "Linear PADRE T Helper Epitope and Carbohydrate B Cell Epitope Conjugates Induce Specific High Titer IgG Antibody Responses," *The Journal of Immunology*, vol. 164, no. 3, pp. 1625–1633, Feb. 2000, DOI: 10.4049/JIMMUNOL.164.3.1625. DOI: <https://doi.org/10.4049/jimmunol.164.3.1625>
 58. H. Ghaffari-Nazari, J. Tavakkol-Afshari, M. R. Jaafari, S. Tahaghoghi-Hajghorbani, E. Masoumi, and S. A. Jalali, "Improving Multi-Epitope Long Peptide

- Vaccine Potency by Using a Strategy that Enhances CD4+ T Help in BALB/c Mice," *PLoS One*, vol. 10, no. 11, Nov. 2015, DOI: 10.1371/JOURNAL.PONE.0142563. DOI: <https://doi.org/10.1371/journal.pone.0142563>
59. D. van der Spoel, E. Lindahl, B. Hess, G. Groenhof, A. E. Mark, and H. J. C. Berendsen, "GROMACS: Fast, flexible, and free," *J Comput Chem*, vol. 26, no. 16, pp. 1701–1718, Dec. 2005, DOI: 10.1002/JCC.20291. DOI: <https://doi.org/10.1002/jcc.20291>
 60. F. Celada and P. E. Seiden, "A computer model of cellular interactions in the immune system," *Immunol Today*, vol. 13, no. 2, pp. 56–62, 1992, DOI: 10.1016/0167-5699(92)90135-T. DOI: [https://doi.org/10.1016/0167-5699\(92\)90135-T](https://doi.org/10.1016/0167-5699(92)90135-T)
 61. R. Puzone, B. Kohler, P. Seiden, and F. Celada, "IMMSIM, a flexible model for in machina experiments on immune system responses," *Future Generation Computer Systems*, vol. 18, no. 7, pp. 961–972, Aug. 2002, DOI: 10.1016/S0167-739X(02)00075-4. DOI: [https://doi.org/10.1016/S0167-739X\(02\)00075-4](https://doi.org/10.1016/S0167-739X(02)00075-4)
 62. S. Gong and R. M. Ruprecht, "Immunoglobulin M: An Ancient Antiviral Weapon – Rediscovered," *Front Immunol*, vol. 11, p. 1943, Aug. 2020, DOI: 10.3389/FIMMU.2020.01943/BIBTEX. DOI: <https://doi.org/10.3389/fimmu.2020.01943>
 63. B. P. O'Connor, M. W. Gleeson, R. J. Noelle, and L. D. Erickson, "The rise and fall of long-lived humoral immunity: terminal differentiation of plasma cells in health and disease," *Immunol Rev*, vol. 194, p. 61, Aug. 2003, DOI: 10.1034/J.1600-065X.2003.00055.X. DOI: <https://doi.org/10.1034/j.1600-065X.2003.00055.x>
 64. F.-M. Lum et al., "Monkeypox: disease epidemiology, host immunity and clinical interventions," *Nature Reviews Immunology* 2022, pp. 1–17, Sep. 2022, DOI: 10.1038/s41577-022-00775-4.
 65. S. C. Johnston et al., "Cytokine modulation correlates with severity of monkeypox disease in humans," *Journal of Clinical Virology*, vol. 63, pp. 42–45, Feb. 2015, DOI: 10.1016/J.JCV.2014.12.001. DOI: <https://doi.org/10.1016/j.jcv.2014.12.001>
 66. F.-M. Lum et al., "Monkeypox: disease epidemiology, host immunity and clinical interventions," *Nature Reviews Immunology* 2022, pp. 1–17, Sep. 2022, DOI: 10.1038/s41577-022-00775-4. DOI: <https://doi.org/10.1038/s41577-022-00775-4>
 67. P. R. Pittman et al., "Clinical characterization of human monkeypox infections in the Democratic Republic of the Congo," *medRxiv*, p. 2022.05.26.22273379, May 2022, DOI: 10.1101/2022.05.26.22273379. DOI: <https://doi.org/10.1101/2022.05.26.22273379>
 68. J. Goulding, G. Abboud, V. Tahiliani, P. Desai, T. E. Hutchinson, and S. Salek-Ardakani, "CD8 T Cells Use IFN- γ To Protect against the Lethal Effects of a Respiratory Poxvirus Infection," *The Journal of Immunology*, vol. 192, no. 11, pp. 5415–5425, Jun. 2014, DOI: 10.4049/JIMMUNOL.1400256/-/DCSUPPLEMENTAL. DOI: <https://doi.org/10.4049/jimmunol.1400256>
 69. F. J. A. de Miranda, I. Alonso-Sánchez, A. Alcamí, and B. Hernaez, "TNF Decoy Receptors Encoded by Poxviruses," *Pathogens* 2021, Vol. 10, Page 1065, vol. 10, no. 8, p. 1065, Aug. 2021, DOI: 10.3390/PATHOGENS10081065. DOI: <https://doi.org/10.3390/pathogens10081065>
 70. P. H. Verardi, L. A. Jones, F. H. Aziz, S. Ahmad, and T. D. Yilma, "Vaccinia virus vectors with an inactivated gamma interferon receptor homolog gene (B8R) are attenuated In vivo without a concomitant reduction in immunogenicity," *J Virol*, vol. 75, no. 1, pp. 11–18, Jan. 2001, DOI: 10.1128/JVI.75.1.11-18.2001. DOI: <https://doi.org/10.1128/JVI.75.1.11-18.2001>
 71. B. Marshall et al., "Variola virus FIL is a Bcl-2-like protein that unlike its vaccinia virus counterpart inhibits apoptosis independent of Bim," *Cell Death & Disease* 2015 6:3, vol. 6, no. 3, pp. e1680–e1680, Mar. 2015, DOI: 10.1038/cddis.2015.52. DOI: <https://doi.org/10.1038/cddis.2015.52>
 72. W. L. Simon, H. M. Salk, I. G. Ovsyannikova, R. B. Kennedy, and G. A. Poland, "Cytokine production associated with smallpox vaccine responses," *Immunotherapy*, vol. 6, no. 10, p. 1097, Oct. 2014, DOI: 10.2217/IMT.14.72. DOI: <https://doi.org/10.2217/imt.14.72>